Çukurova Üniversitesi Mühendislik Fakültesi Dergisi, 38(3), ss. 671-681, Eylül 2023
Cukurova University Journal of the Faculty of Engineering, 38(3), pp. 671-681, September 2023

Analysis of Current Limiting Algorithm with Anti-Windup Control for Transient Stability of Grid-Forming Converters

Özgür ÇELİK[*1] ORCID *0000-0002-7683-2415*

[1]*Adana Alparslan Türkeş Science and Technology University, Faculty of Engineering, Department of Energy Systems Engineering, Adana, Türkiye*

Geliş tarihi: 04.08.2023 Kabul tarihi: 29.09.2023

Atıf şekli/ How to cite: ÇELİK, Ö., (2023). Analysis of Current Limiting Algorithm with Anti-Windup Control for Transient Stability of Grid-Forming Converters. Cukurova University, Journal of the Faculty of Engineering, 38(3), 671-681.

Abstract

In modern power grids, renewable energy sources (RESs) are integrated to the grid through voltage source converters (VSCs) with grid-forming capabilities. Grid forming VSCs' weak overcurrent capability revealed the need for current limiting techniques under large disturbances like short-circuit faults. However, current saturation algorithms induce transient instabilities due to the AC voltage controller windup issue when the current is saturated. Therefore, analyzing the transient stability of the grid-forming units in case of fault conditions is crucial for ensuring the reliable and secure operation of the grid. This paper investigates the effects of the current limiting algorithm with anti-windup control to handle transient instabilities during fault conditions. An elaborated theoretical analysis of the presented system is performed by considering different case studies. The simulations are conducted by using Matlab/Simulink software to test the validity of the presented system. The obtained results highlight the advantages of an anti-windup controller during current saturation mode.

Keywords: VSCs, Grid-forming, Current saturation, Anti-windup, Power flow control

Şebeke-Şekillendirici Dönüştürücülerin Geçici Durum Kararlılığı için Anti-Windup Kontrollü Akım Sınırlama Algoritmasının Analizi

Öz

Modern güç şebekelerinde, yenilenebilir enerji kaynakları (YEK'ler) şebeke oluşturma kabiliyetine sahip gerilim kaynağı dönüştürücüleri (VSC'ler) aracılığıyla şebekeye entegre edilmektedir. Şebeke oluşturan VSC'lerin düşük aşırı akım kapasitesi, kısa devre arızaları gibi büyük bozulmalar altında akım sınırlama tekniklerine olan ihtiyacı ortaya çıkarmıştır. Ancak, akım doyum algoritmaları, akım doyuma ulaştığında AC gerilim kontrolörünün windup sorunu nedeniyle geçici kararsızlıklara neden olur. Bu nedenle, arıza durumlarında şebeke oluşturan birimlerin geçici kararlılığının analiz edilmesi, şebekenin güvenilir ve emniyetli çalışmasını sağlamak için çok önemlidir. Bu makale, arıza koşulları sırasında geçici kararsızlıkların üstesinden gelmek için windup önleyici kontrollü akım sınırlama algoritmasının etkilerini araştırmaktadır. Sunulan sistemin ayrıntılı bir teorik analizi, farklı vaka çalışmaları dikkate alınarak

[*]Sorumlu yazar (Corresponding Author): Özgür ÇELİK, *ozgurcelik@atu.edu.tr*

gerçekleştirilmiştir. Simülasyonlar, sunulan sistemin geçerliliğini doğrulamak için Matlab/Simulink yazılımı kullanılarak gerçekleştirilmiştir. Elde edilen sonuçlar, akım doygunluk modu sırasında bir windup önleyici kontrolörün avantajlarını vurgulamaktadır.

Anahtar Kelimeler: VSCs, Şebeke-şekillendirici, Akım doyum, Anti-windup, Güç akışı kontrolü

1. INTRODUCTION

Increasing energy demand in line with the industrial improvements and growing population paved the way for more common utilization of clean and sustainable energy sources [1,2]. In addition, the energy crisis owing to the exhaustion of fossil fuels and environmental concerns related to carbon emissions make renewable energy sources (RESs) the focus of attention [3]. To interface the RESs with the utility grid voltage source converters (VSCs) are commonly utilized in power networks [4]. Based on their operation, converters can be classified into three main types namely grid-feeding, grid-supporting, and grid-forming [5]. The grid-feeding converter can be described as a controlled current source in parallel with an impedance. On the other hand, the grid-forming converter can be introduced as a controlled voltage source in series with an impedance [6]. The idea behind the grid-feeding converter is synchronization to the grid by employing a phase-locked loop (PLL) and controlling the powers in the outer loop and current in the inner loop. It can be said that the current is limited at the outer control loop which forms reference currents for the inner control loop within the converter operating boundaries [7]. In the grid-forming control, the outer power loops generate operating voltage/phase angle and inner voltage/current loops inject generated power according to references taken from the outer loop [8]. The grid–forming concept is fundamentally proposed for islanded grid applications and uninterruptible power supply applications. Then, this concept is adopted to VSCs-based RESs in line with the increased distributed generation in power grids. It means that there is a control paradigm shift from central control to distributed control for power grids. The grid-forming VSCs have the ability to mimic the behavior of synchronous generators. They can ensure inertial response and fault current contribution to enhancing the grid stability [9]. Due to the behavior as a voltage source, high current overshoots can be experienced during fault transients. It can be said that grid-forming converters are more prone to transient instabilities. Therefore, a current limiting algorithm for grid forming units is mandatory to protect the converter components and maintain the grid stability without having a protective fault tripping [10]. In this manner, current limitation techniques attract attention for grid-forming VSCs. VSCs are allowed to withstand overcurrent up to 20-40% of the rated operation current while the synchronous generators can cope with six-seven times of rated current [11]. There are two main current limitation techniques for grid-forming VSCs highlighted in the literature. These current limitation techniques are basically activated during transients to restrict the current and enhance the transient stability. Among current limitation techniques, the virtual impedance method is one of the more widely used current limitation techniques in the literature [12,13]. The main idea for this method is to apply the effect of impedance in case of current peaks during transients. In [11], authors compared the virtual impedance and current limiting algorithms for short-circuit fault analysis of droop-controlled VSCs. In [12], authors have focused on virtual impedance current limiters to enhance transient stability in event of overload. In [13], Xiong et. al., have revealed the effect of virtual resistance on transient stability and performed design-oriented analysis. In [14], authors have discussed the development of an adaptive virtual impedance current limitation method to ensure effective protection in case of different fault current levels.

The other current limitation technique is the current saturation algorithm [4]. In this technique, whether the d-axis or q-axis can be determined as a priority according to vector orientation and these components can be limited by adjusting a set of equations [11]. In [4], Huang et. al., have discussed the transient stability of droop-controlled VSCs by

taking the current saturation algorithm into account. In [11], authors have performed a comparison between the current limiting techniques and their effect on transient stability. In [15], the current saturation analysis for grid-forming VSC and anti-windup control design has been explained by the authors. In [16], a single-phase grid-connected droop-controlled VSC with a current limiter has been modeled by the authors. In [17], authors have utilized current limiters and investigated interactions between grid-forming converters and synchronous machines. In this paper, the current limiting algorithm with anti-windup control is applied for droop-controlled grid-forming converters. The current limiting algorithm is adopted to the inner current/voltage control loop. Then, the transient behavior of the converter is investigated under large disturbances. Conducted several case results illustrate improved stability and effective protection performance of the analyzed control scheme.

This paper is structured as follows. Droop-controlled grid-forming VSC is given in Section 2. Section 3 describes the developed system. In Section 4, transient analysis of droop-controlled VSC with current limiting algorithm is explained. Performance analysis of the developed system based on the simulation studies is presented in Section 5. Section 6 highlights the conclusions and discussion of this study.

2. DROOP CONTROLLED GRID-FORMING VSC

2.1. Description of the System

The constructed system is illustrated in Figure 1. The system mainly includes two droop-controlled VSC with an LCL filter, two load banks (one is constant other one is controlled), a transformer, and ac grid. The grid is modeled as a three-phase ac voltage source that has equivalent grid impedance. "V_g" represents the grid voltage, "L_{inv}" is the inverter side filter inductance, "L_g" grid side filter inductance, and "C_f" is the filter capacitor. "I_{inv}", "V_{abc}", and "I_{abc}" represent inverter side current, capacitor voltage, and grid side current, respectively.

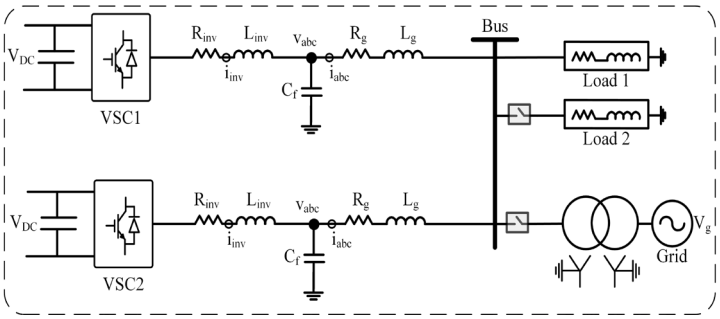

Figure 1. General diagram of the constructed system

2.2. Droop-Controlled Grid-Forming VSC

Grid-forming control acts like a voltage source connected to an impedance as demonstrated in Figure 2. Droop control basically emulates the speed droop feature of the synchronous generator governor. It is possible to mimic the relation between frequency and output power fluctuation. On the other hand, reactive power control is accountable for the voltage magnitude as a voltage regulator.

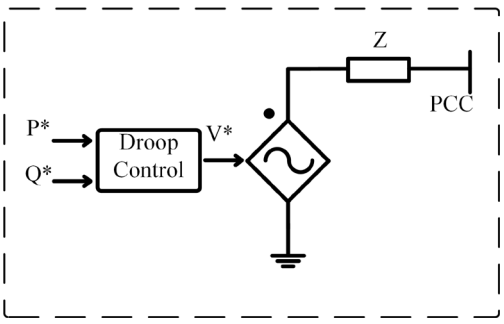

Figure 2. Grid-forming control

The control diagram of the constructed system is depicted in Figure 3. The cascaded inner current/voltage and outer power control loops are included to utilize multi-loop droop control [18].

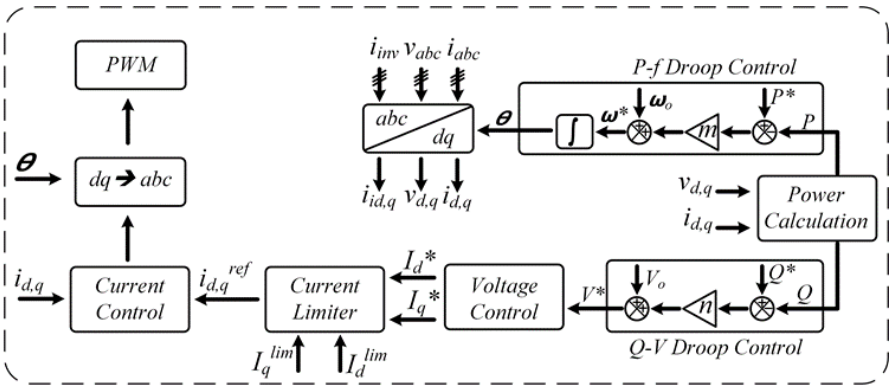

Figure 3. Control scheme of the constructed system

The angular frequency and reference voltage are attained by means of the outer droop control loop. The formulation of the traditional P-f and Q-V droop controls are given in Equations (1) and (2) [19].

$$\omega^* - \omega_o = m(P^* - P) \tag{1}$$

$$V^* - V_o = n(Q^* - Q) \tag{2}$$

where "ω_o" - denotes reference angular frequency, "m" - is the active power droop constant, "V_o" - is the reference voltage, and "n" - is the reactive power droop constant. The inner control structure of the VSC is performed based on the synchronous rotating frame. As depicted in Figure 3, the inverter filter capacitor voltage and output current are measured to calculate instantaneous active/reactive power by applying Park transformation as in Equations (3) and (4) [19].

$$\overline{y_{dq}} = [\, v_{abc}\; i_{abc}]^T \tag{3}$$

$$\left.\begin{aligned} P &= v_{abc,d} * i_{abc,d} + v_{abc,q} * i_{abc,q} \\ Q &= v_{abc,d} * i_{abc,q} - v_{abc,q} * i_{abc,d} \end{aligned}\right\} \tag{4}$$

where "v_{abc}" - is the capacitor voltage, and "i_{abc}" - is the current injected to the grid. The inner voltage/current control loops are included to ensure rapid control of the filter capacitor voltage. Reference value for the voltage control loop is taken from the outer Q-V droop control loop. The reference current nodes are computed by using the feedback terms that passed through the PI controller and adding feed-forward terms as in (5) and (6).

$$\dot{v}_{dq} = v^*_{abc,dq} - v_{abc,dq} \tag{5}$$

$$i^*_{inv,dq} = G_i i_{abc,dq} \mp wC v_{abc,dq} + k_{pv}\dot{v}_{dq} + k_{iv} v_{dq} \tag{6}$$

where "G_i" - is the feedforward constant, "k_{pv}" - is the proportional gain for the voltage controller, and "k_{iv}" is the integral gain for the voltage controller. The computed current reference nodes in the *dq*-frame are then passed through the current limiting block. After that, these reference values are applied to the current control loop to generate internal voltage reference in the *dq*-frame for the PWM block. The current control loop is also performed by using PI controllers and feedback terms as presented in (7) and (8).

$$\dot{i}_{dq} = i^*_{inv,dq} - i_{inv,dq} \tag{7}$$

$$v_{ref,dq} = wLi_{inv,dq} + k_{pc}\dot{i}_{dq} + k_{ic} i_{dq} \tag{8}$$

where "k_{pc}" - is the proportional gain for the current controller and "k_{ic}" is the integral gain for the current controller. The main objective is to design a well-parametrized inner voltage/current loop. In

line with this, it is possible to make inverter filter capacitor voltage behavior as the controllable voltage source [18].

3. CURRENT LIMITING ALGORITHMS AND ANTI-WINDUP CONTROL

3.1. Current Limiting Algorithm

The multiloop control system presented in this paper is oriented to *d*-axis by adjusting the *q*-axis voltage to zero. Therefore, V_d is used as a reference for the required voltage magnitude. In utilized control scheme, reference currents for the current loop are generated by the voltage control loop. In case of an overload situation or short-circuit fault, the current saturation algorithm given in Equation (9) limits the current to protect the VSC from being damaged [4,11,15-17].

$$\left.\begin{aligned} I_d^{ref} &= \min\left(I_{max}, \left|I_d^{ref}\right|\right) \\ I_q^{ref} &= \min\left(\sqrt{{I_{max}}^2 - \left(I_d^{ref}\right)^2}, \left|I_q^{ref}\right|\right) \end{aligned}\right\} \quad (9)$$

Where "I_{max}" - is the maximum allowable current level, [A]; "I_d^{ref}" and "I_q^{ref}" -are the reference current values generated by the inner voltage control loop, [A].

3.2. Presented Anti-Windup Control

In grid-feeding inverters which behave as current-controlled sources, PLL is responsible to notice the grid voltage phase angle, and the detected phase angle is used for park transformation even under conditions that require current limiting. However, in grid-forming control output of the voltage control saturates and is not able to keep the voltage level at the level of grid voltage [12]. It means that in the current saturation situation, the value of Vq is no more equal to zero. Hence, the alignment of the *dq*-axis cannot be maintained. To solve this problem, an anti-windup strategy is applied for the voltage regulators. In this manner, the integral controller gains are dynamically changed to zero during the current saturation mode and alignment of *dq*-axis voltages is ensured. The conditional integration method is applied for anti-windup protection. When the output of the controller reached the saturation limit, the integrator coefficient is adjusted to zero. The schematic of the PI controller with anti-windup protection is illustrated in Figure 4 [20].

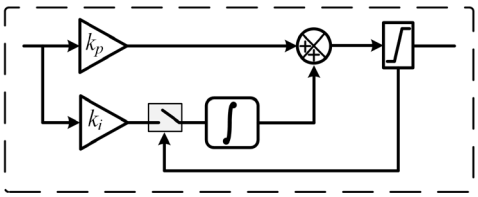

Figure 4. Block diagram of PI controller with anti-windup [20]

In case of abnormal conditions such as overload or severe voltage sags due to short-circuit fault, the current saturation algorithm is triggered. In this manner, by using the PI controller with an anti-windup, the voltage controller windup can be prevented. Thus, it is possible to achieve higher transient stability for the grid-forming VSC.

4. TRANSIENT ANALYSIS OF DROOP-CONTROLLED VSC WITH CURRENT LIMITING ALGORITHM

The transient stability of the droop-controlled grid-forming converter under large disturbances is introduced in this part. In case of large disturbances, it is easy to trigger current saturation and cause a failure at the inner voltage control loop. The applied large-signal disturbances are;

- Symmetrical three-phase short-circuit fault,
- Load variation.

In these cases, the dynamic behavior of the converter is investigated for both inner and outer control loops. When the voltage sag occurs, the droop-controlled VSC behaves like a current source which normally behaves like a voltage source because of the current limitation. This reduces the stability margin. The merits of the current limiting technique on the large-signal transient stability is tried to explain by considering variation in the output power. The active power of VSC in the

current limiting situation can be calculated as in Equation (10).

$$P_{max} = UI_{max}cos\vartheta \tag{10}$$

The VSC can remain in a stable region if the fault is cleared prior to arriving at the power angle limit.

$$\vartheta_{limit} = \text{acos}\,(P/P_{max}) \tag{11}$$

5. RESULTS AND DISCUSSIONS

Performance analysis of the presented system in Figure 1 is conducted in Matlab/Simulink environment to illustrate the advantages of the developed control structure. The parameters for the system simulation are highlighted in Table 1.

Table 1. Parameters of the simulated system

	Parameters	Values
Base values	S_{base}	5 kVA
	V_{base}	400 V_{rms}
	w_{base}	2πf
Grid forming unit	Rated Power	5 kW
	Rated Voltage	400 V
	L_{inv}	0.15 pu
	L_g	0.15 pu
	Cf	2.5 pu
	m	0.05 pu/s
	n	0.2 V/Q
	Load	22.4+j0.01 Ω

To test the validity of the presented control approach two case study is applied. For these case studies the results are taken for control structure without the current limiting algorithm, with the current limiting algorithm, and with the current limiting algorithm plus anti-windup mechanism. The transient analyses of two case studies are conducted based on the load variation and three-phase short circuit fault condition.

5.1. Responses to Three-phase to Ground Short Circuit Fault

In this scenario, a zero impedance three-phase to-ground short circuit fault on the grid side is considered as a case study. Figure 5 shows the output power deviation for one grid-forming controlled VSC under 5 cycles of three-phase short circuit fault duration which correspond to 100 ms fault time. The output power of the grid-forming VSC unit without the current limiting structure that is shown with the red line instantaneously increases to 25 kW and it takes more than 1 s to achieve a steady-state value. In addition, the output power for the control mechanism with the current limiting feature instantaneously goes to 9 kW and it takes 0.5 s to reach a steady-state value. On the other hand, the output power for the unit with the current limiting algorithm plus anti-windup mechanism increases to 9 kW and it takes 0.25 s to reach a steady-state value. It can be obviously seen that without the current saturation algorithm, the maximum active power output exceeds the allowable current saturation level and keeps increasing the output power.

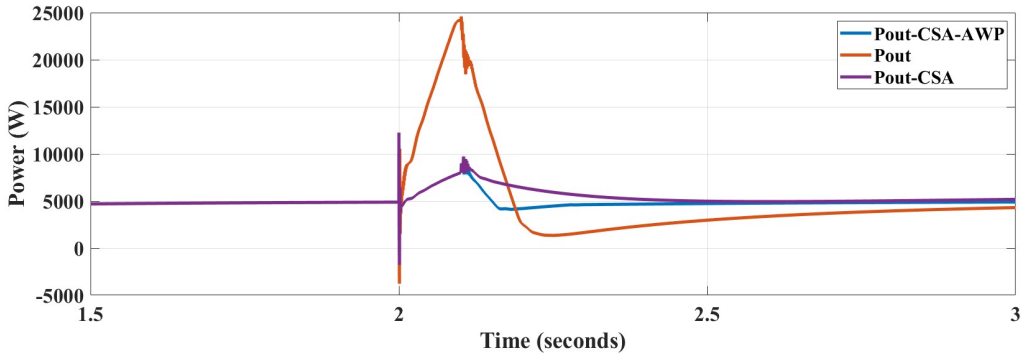

Figure 5. Output power deviation under three-phase short circuit fault

In this event, it is quite normal to lose the synchronization with the grid and not possible to reach a stable equilibrium. However, the current saturation mode helps to keep the converter output power at an allowable rate and reach a stable equilibrium in a short time. It can be noticed also from output current waveforms. The output current waveforms are shown in Figure 6.

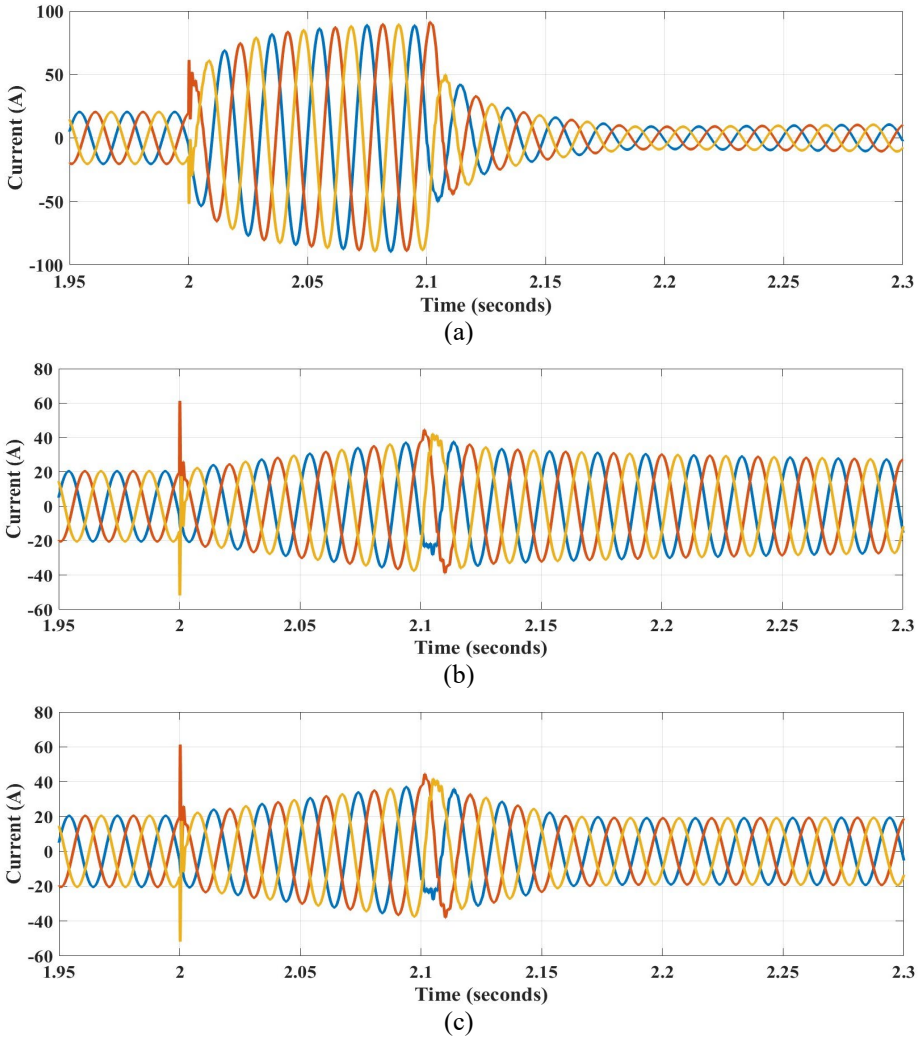

Figure 6. Output current waveforms for grid-forming VSC control structure under short-circuit fault (a) without the current limiting (b) with the current limiting algorithm (c) with the current limiting algorithm plus anti-windup mechanism

The control structure with the current limiting algorithm plus anti-windup mechanism is more robust and stable against the short-circuit fault circumstances. Fault clearing time is also improved thanks to the presented controller structure. To highlight the promising aspects of the presented current limiting control with an anti-windup strategy, the output of the voltage controller is also illustrated in Figure 7.

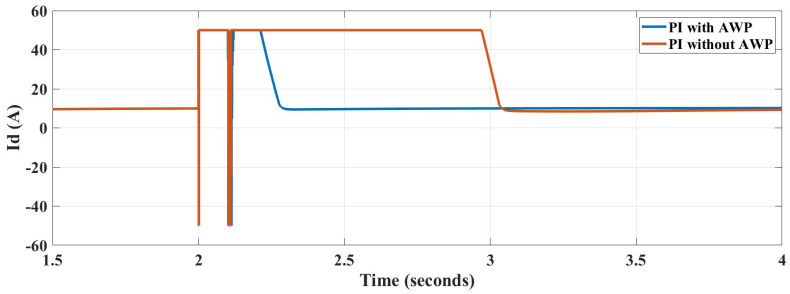

Figure 7. Output of the voltage controller with and without anti-windup protection under three-phase short-circuit fault condition

As depicted in Figure 7, the settling time of the presented current limiting control with an anti-windup control strategy is improved by more than 0.8 s. Hence, the system recovery time in the event of a three-phase short-circuit fault is substantially enhanced. Moreover, it can be concluded that the current saturation algorithm with anti-windup provides transient stability of the system for higher fault durations. The presented is more robust for returning to the normal operation point owing to controlling the integrator of the voltage controller.

5.2. Responses to Load Change

This section discusses the load increment on PCC. It should be noted that a transient instability like in a three-phase to-ground short-circuit fault can also be possible when the grid-forming controlled VSC is subjected to this kind of large disturbance. The load level is instantaneously increased around 4 kW. The increased load level is shared between the units as 2 kW. As can be observed in Figure 8, the output power is more stable in case of the load step change for the control structure with the current saturation algorithm and anti-windup. The VSC unit can come to normal operation much faster than the unit without the current saturation algorithm. In addition, having a control for the integrator of the voltage control enhances the transient stability margin of the system.

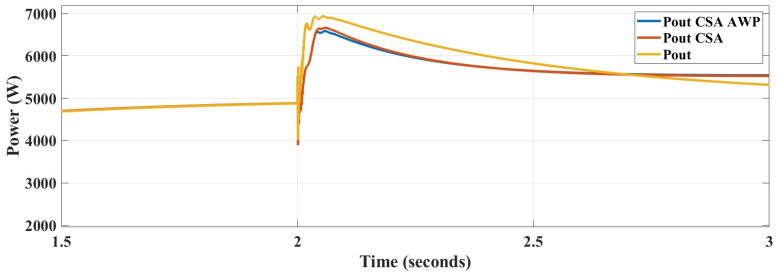

Figure 8. Output power deviation under load change

The output current waveforms are shown in Figure 9. It can be clearly observed that fault clearing time and reaching the stable operation point is remarkably improved for the presented control mechanism. The control structure with the current saturation algorithm and anti-windup maintains transient stability at reasonable operation points and provides stable energy to load according to the demand. However, the VSC without the current saturation algorithm exceeds the stable operation limits and cannot prevent synchronous instability. It means that the VSC without the current saturation algorithm run to a saturated power curve and cannot recover to the stable operation point.

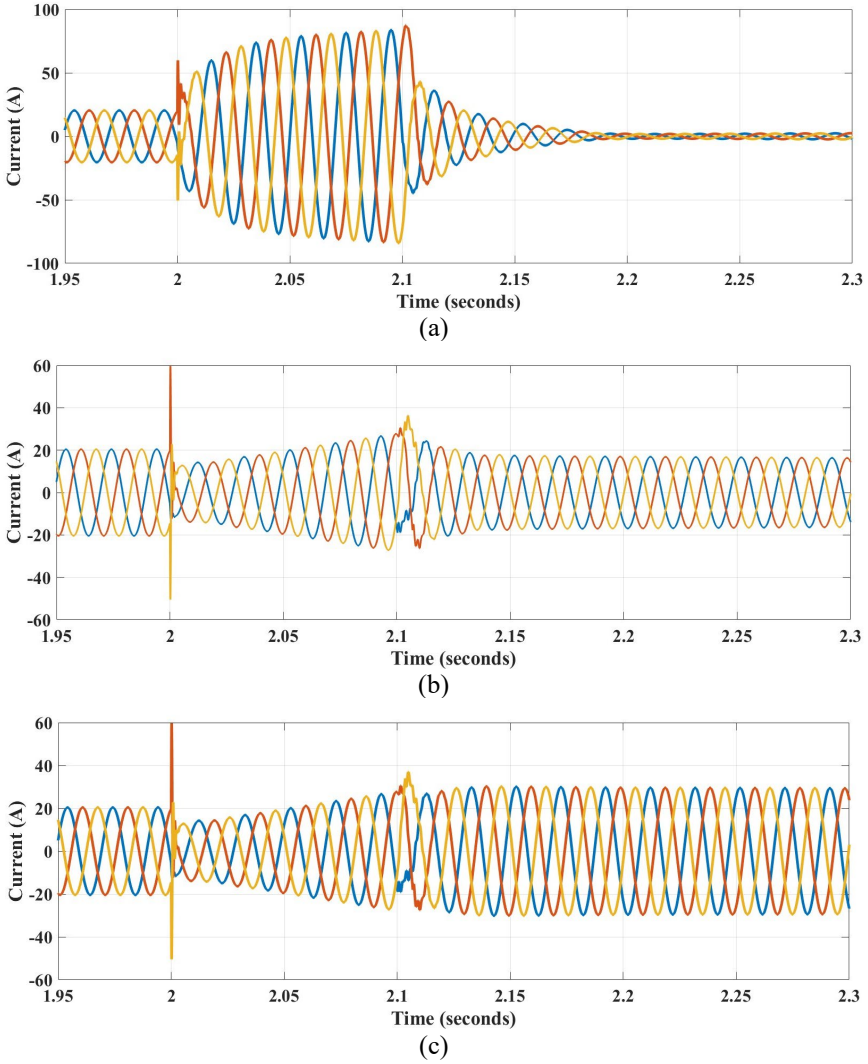

Figure 9. Output current waveforms for grid-forming VSC control structure under load change (a) without the current limiting (b) with the current limiting algorithm (c) with the current limiting algorithm plus anti-windup mechanism

The effect of the anti-windup mechanism can be observed from the output of the voltage controller as shown in Figure 10. It is more robust and stable against load variation circumstances. The controller output recovery time is notably enhanced. Controlling the integrator constant can preserve synchronous stability by preventing unexpected saturation at the output of the voltage controller. The current limiter limits current reference to 50 A. However, without the anti-windup protection, the output of the voltage controller saturates to a defined value and it takes much more time to reach the stable operation point. It can be observed that there is no further increase in the value of integrator output for systems with anti-windup protection and recovery time to normal operation is significantly improved.

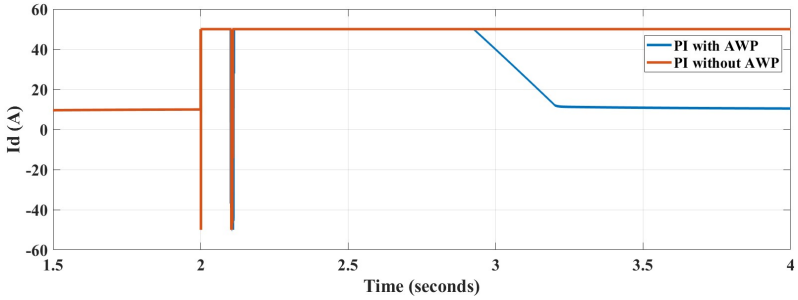

Figure 10. Output of the voltage controller with and without anti-windup protection under load variation

6. CONCLUSION

In this paper, the current saturation algorithm with an anti-windup mechanism for large signal transient stability of droop-controlled VSC is discussed and analyzed in detail. The advantages and limitations of the presented current limiting control with an anti-windup control strategy are highlighted. The presented control structure provides merits in terms of the larger stability margin when compared to the control structure without an anti-windup mechanism. According to the analyzes performed in this study, the anti-windup mechanism is required to preserve synchronous stability by preventing the unexpected saturation at the output of the voltage controller and ensuring fast recovery time to reach normal operation conditions. Otherwise, it takes much time to recover after current saturation and results in a power imbalance in case of using only the current saturation algorithm in the control structure.

6. REFERENCES

1. Çelik, Ö., Zor, K., Tan, A., Teke, A., 2022. A Novel Gene Expression Programming-Based MPPT Technique for PV Micro-Inverter Applications Under Fast-Changing Atmospheric Conditions. Solar Energy, 239, 268-282.

2. Çelik, Ö., Teke, A., Tan, A., 2018. Overview of Micro-Inverters as A Challenging Technology in Photovoltaic Applications. Renewable and Sustainable Energy Reviews, 82, 3191-3206.

3. Reddy, H., Sharma, S., 2021. Implementation of Adaptive Neuro Fuzzy Controller for Fuel Cell Based Electric Vehicles. Gazi University Journal of Science, 34(1), 112-126.

4. Huang, L., Xin, H., Wang, Z., Zhang, L., Wu, K., Hu, J., 2017. Transient Stability Analysis and Control Design of Droop-Controlled Voltage Source Converters Considering Current Limitation. IEEE Transactions on Smart Grid, 10(1), 578-591.

5. Rocabert, J., Luna, A., Blaabjerg, F., Rodriguez, P., 2012. Control of Power Converters in AC Microgrids. IEEE Transactions on Power Electronics, 27(11), 4734-4749.

6. Rosso, R., Wang, X., Liserre, M., Lu, X., Engelken, S., 2020. Grid-Forming Converters: An Overview of Control Approaches and Future Trends. In 2020 IEEE Energy Conversion Congress and Exposition (ECCE), 4292-4299.

7. Zarei, S.F., Mokhtari, H., Ghasemi, M.A., Peyghami, S., Davari, P., Blaabjerg, F., 2019. Control of Grid-Following Inverters Under Unbalanced Grid Conditions. IEEE Transactions on Energy Conversion, 35(1), 184-192.

8. Rosso, R., Wang, X., Liserre, M., Lu, X., Engelken, S., 2021. Grid-Forming Converters: Control Approaches, Grid-Synchronization, and Future Trends-A Review. IEEE Open Journal of Industry Applications, 2, 93-109.

9. Vatta Kkuni, K., 2021. Assessment and Augmentation of Power Converter Control Towards Enhanced Power System Stability. PhD Thesis, Technical University of Denmark.

10. Zhang, L., Harnefors, L., Nee, H.P., 2010. Interconnection of Two Very Weak AC Systems by VSC-HVDC Links using Power-Synchronization Control. IEEE Transactions on Power Systems, 26(1), 344-355.
11. Qoria, T., Gruson, F., Colas, F., Kestelyn, X., Guillaud, X., 2020. Current Limiting Algorithms and Transient Stability Analysis of Grid-Forming VSCs. Electric Power Systems Research, 189, 106726.
12. Paquette, A.D., Divan, D.M., 2014. Virtual Impedance Current Limiting for Inverters in Microgrids with Synchronous Generators. IEEE Transactions on Industry Applications, 51(2), 1630-1638.
13. Xiong, X., Wu, C., Blaabjerg, F., 2021. Effects of Virtual Resistance on Transient Stability of Virtual Synchronous Generators under Grid Voltage Sag. IEEE Transactions on Industrial Electronics, 69(5), 4754-4764.
14. Sati, T.E., Azzouz, M.A., 2022. An Adaptive Virtual Impedance Fault Current Limiter for Optimal Protection Coordination of Islanded Microgrids. IET Renewable Power Generation, 16(8), 1719-1732.
15. Zhuang, K., Xin, H., Hu, P., Wang, Z., 2022. Current Saturation Analysis and Anti-Windup Control Design of Grid-Forming Voltage Source Converter. IEEE Transactions on Energy Conversion, 37(4), 2790-2802.
16. Zhong, Q.C., Konstantopoulos, G.C., 2016. Current-Limiting Droop Control of Grid-Connected Inverters. IEEE Transactions on Industrial Electronics, 64(7), 5963-5973.
17. Tayyebi, A., Groß, D., Anta, A., Kupzog, F., Dörfler, F., 2019. Interactions of Grid-Forming Power Converters and Synchronous Machines. arXiv preprint arXiv, 1902, 10750.
18. Du, W., Chen, Z., Schneider, K.P., Lasseter, R. H., Nandanoori, S.P., Tuffner, F.K., Kundu, S., 2019. A Comparative Study of Two Widely Used Grid-Forming Droop Controls on Microgrid Small-Signal Stability. IEEE Journal of Emerging and Selected Topics in Power Electronics, 8(2), 963-975.
19. Pogaku, N., Prodanovic, M., Green, T.C., 2007. Modeling, Analysis and Testing of Autonomous Operation of an Inverter-Based Microgrid. IEEE Transactions on power electronics, 22(2), 613-625.
20. Ghoshal, A., John, V., 2010. Anti-Windup Schemes for Proportional Integral and Proportional Resonant Controller. National Power Electronıc Conference, 2010.